Mon. Not. R. astr. Soc. (1987) **228,** 427–451

Mode classification and wave propagation in a magnetically structured medium*

S. S. Hasan† *Theoretical Astronomy Unit, School for Mathematical Sciences, Queen Mary College, Mile End Road, London E1 4NS*

Y. Sobouti *Physics Department and Biruni Observatory, Shiraz University, Shiraz, Iran*

Accepted 1987 April 14. Received 1987 April 13; in original form 1987 February 27

Summary. We examine the structure of motions that can occur in a vertical magnetic flux tube with a rectangular cross-section. A polytropic stratification is assumed in the vertical direction. We use a gauged version of Helmholtz's theorem, to decompose the perturbations into an irrotational component and a solenoidal component, which we further split into the sum of poloidal and toroidal components. These components are identified with p, g and toroidal modes of a fluid. The normal modes of the tube are determined using a Rayleigh–Ritz variational technique. Our technique efficiently isolates all the modes to high orders. We first consider some special cases, in order to highlight some interesting properties of the modes. Next, we choose a parameter range to study the properties of oscillations in intense flux tubes on the Sun. Both eigenfrequencies and eigenvectors are determined. It turns out that for intense flux tubes the fundamental is a modified convective mode (g_1 in our notation), whose frequency is in remarkable agreement with the fundamental frequency, obtained from a thin flux tube calculation. For high mode orders, our g modes are essentially slow modes. The t modes are identified with Alfvén waves and the p modes with modified fast waves. We also calculate the height variation of the displacement and pressure perturbations, parallel to the tube axis for the modes. Finally, we discuss some of the observational implications of our study.

1 Introduction

A principal feature of the solar magnetic field, that has been established by observations, is its highly structured form. The field is generally confined to intense flux tubes, with field strengths in the range 1–2 kG at the solar surface (e.g. Stenflo 1973). There exists a hierarchy of structures on the Sun which, despite their widely differing horizontal dimensions, have similar field strengths.

*Contribution No. 14, Biruni Observatory.

†On leave from Indian Institute of Astrophysics, Bangalore, India.

Some examples, in order of decreasing radii, are sunspots, pores, faculae and fibrils. The latter, with diameters typically a few hundred kilometres, are by far the most abundant and the object of the present investigation. However, our analysis is sufficiently general to be applicable to any magnetic structure in a stratified atmosphere.

An understanding of the nature and propagation of waves in magnetic structures is of considerable interest, especially as flux tubes are probably important in heating the chromosphere and corona of the Sun, and more generally of stars. Moreover, the study of waves provides a powerful diagnostic tool for probing various regions of flux tubes, depending on where the waves have maximum amplitude. It is extremely difficult, using ground observations, to detect oscillations in fibrils, chiefly because such observations require extremely good 'seeing', typically, for a few minutes, which is somewhat rare. However, Giovanelli (1975) and Giovanelli, Harvey & Livingston (1978) have reported detection of fibril waves. More observations are clearly needed to learn about the detailed nature of oscillations in fibrils. Till these are available, one must rely mainly on theoretical calculations for understanding physical conditions in fibrils. For sunspots, however, the situation is more favourable. Oscillations in the umbra of sunspots have been detected by numerous observers [see Moore (1981) for a review, Lites & Thomas (1985) and references therein]. Thus an analysis of wave modes in a flux tube would also be applicable to sunspots, although the present study is chiefly concerned with solar fibrils.

Theoretically, the normal modes of an unstratified plane parallel medium with a uniform magnetic field are well known (e.g. Ferraro & Plumpton 1966). For an ideal fluid, initially at rest, these are the usual fast, slow and Alfvén modes. The inclusion of gravity greatly complicates the analysis and a straightforward classification is possible only under certain idealized simplifications (Lighthill 1967). Qualitatively, one expects the introduction of an extra force to generate an additional mode, which in the present case is driven by gravity. The normal modes are sensitive to the interplay among the forces of pressure, gravity and magnetic field, thus rendering a general analysis fairly difficult. Nevertheless, many authors have examined the behaviour of magneto–acoustic–gravity waves (MAG for short). The earlier investigations (McLellan & Winterberg 1968; Bel & Mein 1971; Nagakawa, Priest & Wellck 1973) used a local analysis, which is meaningful for wavelengths which are less than the local pressure scale height. Local dispersion relations and their applicability have been critically discussed by Thomas (1982). Much work has been done on extending the previous analyses of MAG waves to the non-local analysis case (e.g. Antia & Chitre 1978; Schwartz & Bel 1984; Zhugzhda & Dzhalilov 1984). An assumption, which is implicit in these studies, is that the magnetic field is unbounded in the horizontal direction. Some progress has been made in understanding the normal modes of structured magnetic fields (i.e. flux tubes) by using a thin flux tube approximation (Defouw 1976; Roberts & Webb 1978; Spruit & Zweibel 1979; Spruit 1982; Hasan 1986), which neglects variations in physical quantities transverse to the direction of the magnetic field. Although, this approximation is often adequate below the photosphere, it breaks down in the upper layers, where the radius of the flux tube becomes comparable to or even greater than the local pressure scale height. Furthermore, it gives incomplete information on the modal structure. It provides a reasonable estimate to the low-frequency magnetogravity modes, but automatically excludes the Alfvén and fast modes. In the present examination we shall not employ this approximation.

The modes of a magnetic slab, without gravity, have been investigated amongst others by (Parker 1974; Cram & Wilson 1975; Wilson 1979; Wentzel 1979; Roberts 1981a, b; Edwin & Roberts 1982, 1983; Cally 1985a, b). A general analysis for a stratified medium (i.e. including gravity) does not appear to have been carried out in the context of solar fibrils. The interaction of gravity with magnetic fields is likely to be important in the upper convection zone of the Sun and may be responsible for flux tube formation (Parker 1978; Webb & Roberts 1978; Spruit 1979; Hasan 1984a, b).

We use a variational technique following Chandrasekhar (1964) and Sobouti (1977a, 1981), which has the advantage that it permits from the very outset, a natural decomposition of the perturbations into pressure (p), gravity (g) and Alfvén (t) modes. This considerably simplifies the task of mode classification. We shall make a few simplifying assumptions, so as to highlight the physical nature of the modes. In particular, we treat only body oscillations and exclude surface waves from the present analysis, deferring them and the use of more general boundary conditions to subsequent papers.

Our paper is divided as follows: in Section 2 we present the ideal MHD equations, which we linearize and cast in a form suitable for a variational analysis. In Section 3, we generate suitable decompositions for the perturbed quantities into p, g and t components, derived from scalar potentials, and consider specific forms for these potentials in Section 4. The variational technique is outlined in Section 5, which transforms the equations into a generalized eigenvalue problem. Some properties of the matrices, which appear in the final equations, are discussed in Sections 6 and 7. Analytic solutions are presented in Section 8. The numerical technique and results for a stratified medium are given in Section 9, followed by an application to intense flux tubes in Section 10. Section 11 consists of a discussion and some observational implications of the results and the final Section 12 has concluding remarks.

2 Equations

Let us consider a single flux tube of rectangular cross-section extending vertically into the solar convection zone. We adopt a Cartesian coordinate system with the z axis parallel to the tube axis and pointing into the Sun. For convenience we choose the origin at one of the tube corners, with $z=0$ at the base of the photosphere. Let the tube have sides a, b and d in the x, y and z directions respectively. Furthermore, we assume that the flux tube has a uniform field B (constant with depth) and that the field outside the tube is zero. From the principle of flux conservation, the cross-sectional area must also be constant with depth.

The ideal MHD equations are

$$\frac{\partial \varrho}{\partial t} + \operatorname{div}(\varrho \mathbf{v}) = 0 \tag{1}$$

$$\varrho \frac{d\mathbf{v}}{dt} = \varrho \mathbf{g} - \nabla P + \frac{1}{4\pi} \operatorname{curl} \mathbf{B} \times \mathbf{B} \tag{2}$$

$$\frac{d}{dt}\left(\frac{P}{\varrho^{\gamma}}\right) = 0 \tag{3}$$

$$\operatorname{div} \mathbf{B} = 0 \tag{4}$$

$$\operatorname{curl} \mathbf{E} = -\frac{1}{c}\frac{\partial \mathbf{B}}{\partial t} \tag{5}$$

$$\mathbf{E} + \frac{1}{c}(\mathbf{v} \times \mathbf{B}) = 0 \tag{6}$$

where the unknowns are ϱ, $\mathbf{v}$, P and $\mathbf{B}$, which refer to density, velocity, pressure and magnetic field respectively. The constants $\mathbf{g}$, c and γ represent the acceleration due to gravity, the speed of light and the ratio of specific heats respectively.

We have assumed (see equation 3) that all changes occur adiabatically and that the medium has infinite electrical conductivity.

2.1 EQUILIBRIUM EQUATIONS

Initially (at $t=0$), let us assume a polytropic fluid in the flux tube, which is in hydrostatic equilibrium. Furthermore, we assume that all equilibrium quantities depend only on z, apart from **B** which we assume to be constant both in direction and magnitude. Thus, in equilibrium we have

$$\frac{dP}{dz}=\varrho g \tag{7}$$

$$P=P_0\left(\frac{\varrho}{\varrho_0}\right)^{1+1/n} \tag{8}$$

where n is the polytropic index and the subscript '0' refers to values at $z=0$. From equations (7) and (8), we have

$$\varrho=\varrho_0\left[1+\frac{z}{(n+1)h}\right]^n \tag{9}$$

where $h=P_0/\varrho_0 g$ is the scale height of the atmosphere at $z=0$. The temperature T follows from equations (8)–(9) and assuming the ideal gas law to be

$$T=T_0\left[1+\frac{z}{(n+1)h}\right]. \tag{10}$$

We relate physical variables inside the flux tube with those in the external medium by assuming that the total pressure at the interface (the planes $x=0$, a and $y=0$, b) is continuous, so that

$$P+\frac{B^2}{8\pi}=P_e. \tag{11}$$

Thus, by specifying both P and B, we automatically determine P_e, the external pressure at the interface. If we assume, furthermore, that the gas outside is also in hydrostatic equilibrium, it follows that

$$\varrho=\varrho_e \tag{12}$$

and

$$T_e=T\left\{1+\frac{1}{\beta}\left[1+\frac{z}{(n+1)h}\right]^{-(n+1)}\right\} \tag{13}$$

where $\beta=8\pi P_0/B^2$. In this case, the gas outside has the same density, but a higher temperature than the gas inside.

2.2 LINEARIZED EQUATIONS

Let $\boldsymbol{\xi}(\mathbf{x}, t)$ denote a small Lagrangian displacement of a fluid mass element from its equilibrium position. Equations (1)–(6) after linearization yield

$$\varrho\frac{\partial^2\boldsymbol{\xi}}{\partial t^2}=-\mathbf{F}(\boldsymbol{\xi}) \tag{14}$$

with

$$\mathbf{F}(\xi)=\nabla\delta P-\delta\varrho\mathbf{g}-\frac{1}{4\pi}\,\mathrm{curl}\;\delta\mathbf{B}\times\mathbf{B} \tag{15}$$

$$\delta\varrho=-\varrho\;\mathrm{div}\;\xi-\xi\cdot\nabla\varrho \tag{16}$$

$$\delta P=-\gamma P\;\mathrm{div}\;\xi-\xi\cdot\nabla P \tag{17}$$

$$\delta\mathbf{B}=\mathrm{curl}\;(\xi\times B) \tag{18}$$

$$\mathbf{v}=\frac{\partial\xi}{\partial t}\,. \tag{19}$$

δf denotes the Eulerian perturbation in the variable f. On multiplying equation (14) by ξ^* and integrating over the volume initially occupied by the flux tube, we obtain

$$\omega^2\int d\mathbf{x}\;\xi^*\cdot\varrho\xi=\int d\mathbf{x}\;\xi^*\cdot\mathbf{F}(\xi)=\int d\mathbf{x}\left[\xi^*\cdot\nabla\delta P-\xi^*\cdot\mathbf{g}\delta\varrho-\frac{1}{4\pi}\,\xi^*\cdot\mathrm{curl}\;\delta\mathbf{B}\times\mathbf{B}\right] \tag{20}$$

where we have assumed ξ to have a time dependence proportional to $\exp(i\omega t)$.

An integration by parts of the first and last terms on the right-hand side of equation (20) and using equation (7) yields

$$\int d\mathbf{x}\;\xi^*\cdot\mathbf{F}(\xi)=\int d\mathbf{x}\left[-\mathrm{div}\;\xi^*\delta P-\xi^*\cdot\frac{\nabla P}{\varrho}\delta\varrho+\frac{\delta\mathbf{B}}{4\pi}\cdot\mathrm{curl}\;(\xi^*\times\mathbf{B})\right]$$
$$+\int dS\;\mathbf{n}\cdot\left[\xi^*\delta P+\frac{1}{4\pi}\,\delta\mathbf{B}\times(\xi^*\times\mathbf{B})\right] \tag{21}$$

where $\mathbf{n}$ is a unit normal pointing outward from the surface S. From equations (16) and (17) and noting that for a polytrope $P=P(\varrho)$, we have

$$\delta P=\frac{dP}{d\varrho}\,\delta\varrho-\alpha P\;\mathrm{div}\;\xi \tag{22}$$

where

$$\alpha=\gamma-\frac{\varrho}{P}\,\frac{dP}{d\varrho}\,. \tag{23}$$

Substituting equation (22) into equation (21). We have

$$\int d\mathbf{x}\;\xi^*\cdot\mathbf{F}(\xi)=\int d\mathbf{x}\left(\frac{1}{\varrho}\,\frac{dP}{d\varrho}\,\delta\varrho^*\;\delta\varrho+\alpha P\;\mathrm{div}\;\xi^*\;\mathrm{div}\;\xi+\frac{1}{4\pi}\,\delta\mathbf{B}^*\cdot\delta\mathbf{B}\right)$$
$$+\int dS\left[(\mathbf{n}\cdot\xi^*)\;\delta P+\frac{1}{4\pi}\,(\mathbf{n}\cdot\xi^*)(\mathbf{B}\cdot\delta\mathbf{B})-\frac{1}{4\pi}\,(\mathbf{B}\cdot\mathbf{n})(\xi^*\cdot\delta\mathbf{B})\right] \tag{24}$$

where we have used equations (16) and (18). The volume integral on the right-hand side of equation (24) is symmetric with respect to ξ and ξ^*. On the planes $z=0$ and $z=d$, we assume that $\xi_z=0$ and therefore the contributions to the surface integrals from these surfaces is zero.* At the interface of the flux tube and external medium we assume the boundary condition given by equation (11), which must hold both in the equilibrium and perturbed states. Thus, equation (11)

*See note added in proof.

must also be valid for the Lagrangian changes associated with the displacement ξ. This yields

$$-\gamma P \operatorname{div} \xi+\frac{1}{4\pi}\mathbf{B}\cdot[\delta\mathbf{B}+(\xi\cdot\nabla)\,\mathbf{B}]=\xi\cdot\nabla P_e \tag{25}$$

where we have neglected the Eulerian change in P_e. Substituting equation (25) into the last integral in equation (24) yields

$$\int dS\,(\mathbf{n}\cdot\xi^*)\left[\delta P+\frac{1}{4\pi}\mathbf{B}\cdot\operatorname{curl}(\xi\times\mathbf{B})\right]=\int dS\,(\mathbf{n}\cdot\xi^*)\,\xi\cdot\nabla\left(P_e-\frac{B^2}{8\pi}-P\right)=0$$

by virtue of equation (11).

Thus, the frequency ω can be determined by solving the following equation

$$w-\omega^2 s=0 \tag{26}$$

where

$$s=\int d\mathbf{x}\,\varrho\xi^*\cdot\xi \tag{27}$$

$$w=w(1)+w(2)+w(3) \tag{28}$$

$$w(1)=\int d\mathbf{x}\frac{1}{\varrho}\frac{dP}{d\varrho}\delta\varrho^*\,\delta\varrho \tag{29}$$

$$w(2)=\int d\mathbf{x}\,\alpha P \operatorname{div}\xi^* \operatorname{div}\xi \tag{30}$$

$$w(3)=\frac{1}{4\pi}\int d\mathbf{x}\,\delta\mathbf{B}^*\cdot\delta\mathbf{B}. \tag{31}$$

From equation (27), s is symmetric and positive definite ($\varrho>0$).Therefore, we may write $\omega^2=w/s$. From equation (29), $w(1)$ is symmetric and positive ($dp/d\varrho>0$). It can be zero if and only if $\delta\varrho=0$, which is possible if $\varrho\xi$ is solenoidal. Thus, $w(1)$ contributes positively to ω^2. From equation (30), $w(2)$ is symmetric and positive for convectively stable fluids, i.e. when $\alpha=\gamma-(P/\varrho)\,dP/d\varrho>0$. It is zero for convectively neutral fluids ($\alpha=0$) and also for solenoidal motions (div $\xi=0$). For convectively unstable fluids ($\alpha<0$), $w(2)$ contributes negatively. Thus the contribution of $w(2)$ to ω^2 may be positive, zero or negative. From equation (31), $w(3)$ is symmetric and positive, unless $\delta\mathbf{B}=0$, when it vanishes. Therefore, $w(3)$ also contributes positively to ω^2. The sum w is symmetric, thus ruling out either damping or overstability. There is, however, the possibility of dynamical instability if the fluid is convectively unstable.

From the point of view of dynamics, separation of ω into three terms has an interesting interpretation. Linear motions of the magnetized fluid are driven by three forces of distinct nature: (a) pressure forces acting through $w(1)$, (b) buoyancy forces acting through $w(2)$, and (c) magnetic forces giving rise to $w(3)$.

Equation (14) or its equivalent variational form (26) constitute a generalized eigenvalue problem. In the next section, we use a 'gauged' version of Helmholtz's theorem to decompose ξ into one irrotational component, one 'weighted solenoidal' poloidal component and one solenoidal toroidal component. These components can be identified with p, g and toroidal modes of a fluid.

3 Decomposition of Lagrangian displacements

Let $\zeta(\mathbf{x}, t)$ denote a linear displacement in the fluid, which need not satisfy equation (26). The collection of all such displacements will belong to a Hilbert space H. We define the inner product in H of ζ and ζ' as

$$(\zeta, \zeta') = \int d\mathbf{x}\, \varrho \zeta^* \cdot \zeta'; \qquad \zeta, \zeta' \in H \tag{32}$$

where the integration is over the volume of the flux tube. This inner product is the same as s (equation 27). By a suitable gauge transformation, ζ can be decomposed using Helmholtz's theorem as follows (Sobouti 1981)

$$\varrho\zeta = -\varrho\nabla\chi_p + \text{curl } \mathbf{A}, \qquad \text{div } \mathbf{A} = 0 \tag{33}$$

where $\chi_p(\mathbf{x})$ is a scalar potential and $\mathbf{A}(\mathbf{x})$ is a divergence-free vector potential. The reason for inclusion of ϱ in equation (33) will emerge when we discuss orthogonality in H. The decomposition in equation (33) is unique and complete.

The solenoidal vector $\mathbf{A}$ can be split further into toroidal and poloidal components: $\mathbf{A} = \text{curl } (\mathbf{k}\chi_g) + \text{curl curl } (\mathbf{k}\chi_t)$, where $\mathbf{k}$ is a unit vector along the z direction. This decomposition is not unique. It is complete, however, in the sense that any solenoidal vector can be broken in this manner. Consequently, we can write

$$\zeta = \zeta_p + \zeta_g + \zeta_t \tag{34}$$

where

$$\zeta_p = -\nabla\chi_p = -\left(\frac{\partial\chi_p}{\partial x}, \frac{\partial\chi_p}{\partial y}, \frac{\partial\chi_p}{\partial z}\right) \tag{35}$$

$$\zeta_g = \frac{1}{\varrho}\,\text{curl curl } (\mathbf{k}\chi_g) = \frac{1}{\varrho}\left[\frac{\partial^2\chi_g}{\partial x\partial z}, \frac{\partial^2\chi_g}{\partial y\partial z}, -\left(\frac{\partial^2}{\partial x^2} + \frac{\partial^2}{\partial y^2}\right)\chi_g\right] \tag{36}$$

$$\zeta_t = \frac{1}{\varrho}\,\text{curl curl curl } (\mathbf{k}\chi_t) = \frac{1}{\varrho}\left(-\frac{\partial}{\partial y}\nabla^2\chi_t, \frac{\partial}{\partial x}\nabla^2\chi_t, 0\right). \tag{37}$$

The irrotational motions ζ_p are associated with substantial changes in pressure and density, and are driven by forces arising from their imbalance. Therefore, the ζ_p motions constitute the dominant components of acoustic or p modes.

For ζ_g motions div $(\varrho\zeta_g) = 0$. We shall refer to them as 'weighted' solenoidal or for brevity only as solenoidal fields. They are poloidal as well. In a fluid of uniform density and pressure or in convectively neutral fluids $(dP/d\varrho = [dP/d\varrho]_{\text{ad}})$, these displacements do not disturb the equilibrium state and remain neutral motions. For a stratified fluid that is convectively non-neutral, however, they induce weak perturbations and give rise to g or convective modes.

Motions of the type ζ_t are toroidal in the sense that they are confined to the x–y plane. With or without the 'weight' ϱ, they are solenoidal, $\text{div}(\varrho\zeta_t) = \text{div}(\zeta_t) = 0$. They do not perturb the equilibrium (even for a stratified medium) and are, therefore, neutral in the absence of magnetic forces. In the presence of a magnetic field, however, toroidal motions induce restoring Lorentz forces, which give rise to Alfvén waves.

So far we have introduced several trios, namely $\{w(1), w(2), w(3)\}$, $\{\zeta_p, \zeta_g, \zeta_t\}$ and $\{p \text{ modes}, g \text{ modes}, t \text{ modes}\}$. There is a close one-to-one correspondence between the members of these trios. It is tempting to suggest a group structure and to consider them as equivalent representations of one another in the group theoretic sense of the word. One of us (YS) is exploring this analogy further, and the results will appear elsewhere.

3.1 ORTHOGONALITY OF p, g AND t DISPLACEMENTS

An immediate conclusion to follow from equations (34)–(37) is the subdivision of the Hilbert space H into three orthogonal subspaces H_p, H_g and H_t, with elements ζ_p, ζ_g and ζ_t respectively. The orthogonality of H_p with respect to H_g and H_t is seen from

$$\int d\mathbf{x}\,\varrho\zeta_p^*\cdot\zeta_{g,t}=-\int d\mathbf{x}\,\nabla\chi_p^*\cdot\operatorname{curl}\mathbf{A}=\int d\mathbf{x}\,\chi_p^*\operatorname{div}\operatorname{curl}\mathbf{A}=0. \tag{38}$$

The orthogonality of H_g with respect to H_t is seen from

$$\int d\mathbf{x}\,\varrho\zeta_g^*\cdot\zeta_t=\int d\mathbf{x}\frac{1}{\varrho}\left(-\frac{\partial^2\chi_g^*}{\partial x\partial z}\frac{\partial}{\partial y}\nabla^2\chi_t+\frac{\partial^2\chi_g^*}{\partial y\partial z}\frac{\partial}{\partial x}\nabla^2\chi_t\right)=0. \tag{39}$$

That the integral in equation (39) vanishes follows from an integration by parts and noting that ϱ is independent of x and y.

4 Ansatz for the scalar potentials

We consider displacements, which have vanishing normal components on the boundaries, i.e. on the planes $z=0, d$; $x=0, a$ and $y=0, b$. At the lower boundary (the plane $z=d$), this choice may be reasonable, if the bottom of the tube is sufficiently deep, so that the density is high enough. The assumption of perfectly reflecting boundaries, however, is not crucial to the analysis and has been made primarily for mathematical convenience.

4.1 ANSATZ FOR THE p MOTIONS

We assume the following choice for the scalar p potential

$$\chi_p^{ijk}=\left(\frac{2}{abd}\right)^{3/2}\cos\left(\frac{\pi ix}{a}\right)\cos\left(\frac{\pi jy}{b}\right)\cos\left(\frac{\pi kz}{d}\right).$$

It is convenient to normalize all lengths by some fixed quantity, say l_0. Let $l_0=d/\pi$, and redefine χ_p as

$$\chi_p^{i'j'k}=\left(\frac{2}{\pi}\right)^{3/2}\cos(i'x)\cos(j'y)\cos(kz) \tag{40}$$

where $i'=i(d/a)$ and $j'=j(d/b)$. Henceforth, the primes on i and j will be dropped. The integers i and j turn out to be the horizontal wavenumbers of an eigensolution ξ of equation (14). Due to the stratification in the z direction, however, the third integer k is not a wavenumber. A superposition of terms with different k is required to construct an eigensolution. For brevity, only the k designation is retained. Using equations (16)–(18) and (35) yields

$$\zeta_p^k=\left(\frac{2}{\pi}\right)^{3/2}[i\sin(ix)\cos(jy)\cos(kz),\ j\cos(ix)\sin(jy)\cos(kz),$$
$$k\cos(ix)\cos(jy)\sin(kz)] \tag{41}$$

$$\operatorname{div}\zeta_p^k=(i^2+j^2+k^2)\,\chi_p^k \tag{42}$$

$$\delta\varrho_p^k=-\varrho\operatorname{div}\zeta_p^k-\left(\frac{2}{\pi}\right)^{3/2}\varrho' k\cos(ix)\cos(jy)\sin(kz) \tag{43}$$

$$\delta\mathbf{B}_p^k=-\left(\frac{2}{\pi}\right)^{3/2}B[ik\sin(ix)\cos(jy)\sin(kz),\ jk\cos(ix)\sin(jy)\sin(kz),$$
$$(i^2+j^2)\cos(ix)\cos(jy)\cos(kz)] \tag{44}$$

where $\varrho' = d\varrho/dz$. The displacement ζ_p^k satisfies the boundary conditions. The completeness of the set $\{\zeta_p^k\}$ in the subspace H_p follows from the completeness of the trigonometric functions used in equation (40). This set will be used as a basis for H_p. Note, however, that the set is not orthonormal in the sense of equation (32).

4.2 ANSATZ FOR g MOTIONS

In what follows ϱ_0, the density at $z=0$ is introduced to keep the dimensions of ζ_g the same as that of ζ_p. Using the same normalization for length as the previous section, we choose

$$\chi_g^k = \left(\frac{2}{\pi}\right)^{3/2} \varrho_0 \cos(ix) \cos(jy) \sin(kz) \tag{45}$$

$$\zeta_g^k = \left(\frac{2}{\pi}\right)^{3/2} \frac{\varrho_0}{\varrho} [-ik \sin(ix) \cos(jy) \cos(kz), -jk \cos(ix) \sin(jy) \cos(kz),$$
$$(i^2+j^2) \cos(ix) \cos(jy) \sin(kz)] \tag{46}$$

$$\operatorname{div} \zeta_g^k = -\left(\frac{2}{\pi}\right)^{3/2} (i^2+j^2) \frac{\varrho_0 \varrho'}{\varrho^2} \cos(ix) \cos(jy) \sin(kz) \tag{47}$$

$$\delta\varrho_g^k = 0 \tag{48}$$

$$\delta \mathbf{B}_g^k = \left(\frac{2}{\pi}\right)^{3/2} \frac{k\varrho_0 B}{\varrho} \left\{ i \sin(ix) \cos(jy) \left[k \sin(kz) + \frac{\varrho'}{\varrho} \cos(kz) \right], \right.$$
$$j \cos(ix) \sin(jy) \left[k \sin(kz) + \frac{\varrho'}{\varrho} \cos(kz) \right],$$
$$\left. (i^2+j^2) \cos(ix) \cos(jy) \cos(kz) \right\}. \tag{49}$$

It may be noted that $\delta\varrho_g$ vanishes and that div ζ_g depends on ϱ'. The implication is that ζ_g motions induce no pressure forces. They do, however, contribute to buoyancy and magnetic forces. This is in contrast to $\delta\varrho_p$ and div ζ_p, which can be fairly large. Like before, $\{\zeta_g^k\}$ is complete in H_g and will be used as a basis.

4.3 ANSATZ FOR t MOTIONS

In equation (37) and the subsequent equations, only the combination $\nabla^2\chi_t/\varrho$ and its x and y derivatives appear. Since ϱ is not a function of x and y, the combination $\nabla^2\chi_t/\varrho$ is redefined and denoted by χ_t. We choose

$$\chi_t^k = \left(\frac{2}{\pi}\right)^{3/2} \sin(ix) \sin(jy) \cos(kz) \tag{50}$$

$$\zeta_t^k = \left(\frac{2}{\pi}\right)^{3/2} [j \sin(ix) \cos(jy) \cos(kz), -i \cos(ix) \sin(jy) \cos(kz), 0] \tag{51}$$

$$\operatorname{div} \zeta_t^k = 0 \tag{52}$$

$$\delta\varrho_t^k = 0 \tag{53}$$

$$\delta \mathbf{B}_t^k = \left(\frac{2}{\pi}\right)^{3/2} B[-jk \sin(ix) \cos(jy) \sin(kz), ik \cos(ix) \sin(jy) \sin(kz), 0]. \tag{54}$$

It may be noted that both $\delta\varrho_t$ and div ζ_t vanish, implying that there are no pressure and buoyant forces. This ensures the neutrality of toroidal motions in the non-magnetic case. The presence of a magnetic field, however, will drive Alfvén waves, thereby generating t motions. Once again $\{\zeta_t^k\}$ complete in H_t and can be used as a basis set.

5 Matrix representation in H

We give a brief description of the procedure used to construct a solution of equation (26). For details, the reader may consult Sobouti (1977a, b and 1986). Let ξ_i be a vector in H and denote an eigensolution of equation (14) or its equivalent (26), corresponding to the eigenvalue $\omega^2=\varepsilon_i$. The subscript i completely specifies the eigensolution in terms of p, g or t and all three wavenumbers. Let $\{\zeta_j\}$ be a basis for H, where j has the same meaning as i. Expanding ξ_i in terms of $\{\zeta_j\}$, we have

$$\xi_i=\sum_j \zeta_j Z_{ji} \tag{55}$$

where Z_{ji} are constants of expansion, which will be treated as variational parameters. Substituting equation (55) in equations (26)–(28) and using a variational technique to minimize the eigenvalues, gives the following matrix equations (Sobouti 1977a)

$$\mathbf{WZ}=\mathbf{SZE} \tag{56}$$

where $\mathbf{E}$ is a diagonal matrix, whose elements are the eigenvalues ε_i and $\mathbf{Z}=[Z_{ji}]$ is the matrix of the variational constants. The elements of $\mathbf{S}$ and $\mathbf{W}$ are (using equations 27–30)

$$S_{ij}=\int d\mathbf{x}\,\varrho\zeta_i^*\cdot\zeta_j \tag{57}$$

$$W_{ij}=W_{ij}(1)+W_{ij}(2)+W_{ij}(3) \tag{58}$$

$$W_{ij}(1)=\int d\mathbf{x}\,\frac{1}{\varrho}\,\frac{dP}{d\varrho}\,\delta\varrho_i^*\delta\varrho_j \tag{59}$$

$$W_{ij}(2)=\int d\mathbf{x}\,\alpha P\ \mathrm{div}\,\zeta_i^*\mathrm{div}\,\xi_j \tag{60}$$

$$W_{ij}(3)=\frac{1}{4\pi}\int d\mathbf{x}\,\delta\mathbf{B}_i^*\cdot\delta\mathbf{B}_j. \tag{61}$$

Thus, given a basis $\{\zeta_j\}$, the $\mathbf{S}$ and $\mathbf{W}$ matrices can be calculated. A solution of equation (56) will then consist of finding $\mathbf{E}$ and $\mathbf{Z}$. The $\mathbf{Z}$ matrix simultaneously diagonalizes $\mathbf{S}$ to the unit matrix and $\mathbf{W}$ to $\mathbf{E}$. Thus,

$$\mathbf{Z}^+\mathbf{WZ}=\mathbf{E}, \tag{62a}$$

$$\mathbf{Z}^+\mathbf{SZ}=\mathbf{I}. \tag{62b}$$

The proof is straightforward and is given in Appendix A1.

5.1 PARTITIONING OF MATRICES

The basis for H will be partitioned as follows: $\{\zeta_p^k\,|\,\zeta_g^l\,|\,\zeta_t^m\}$; $k, l, m=1, 2, \ldots$. The various blocks are given in equations (41), (46) and (51). We partition the matrices of equation (56) into blocks

specified by pp, pg etc. Thus,

$$\mathbf{M}=\begin{bmatrix} M_{pp} & M_{pg} & M_{pt} \\ M_{gp} & M_{gg} & M_{gt} \\ M_{tp} & M_{tg} & M_{tt} \end{bmatrix} \tag{63}$$

where $\mathbf{M}=\mathbf{E}, \mathbf{Z}, \mathbf{W}, \mathbf{S}$. Some of the blocks from every matrix are zero as we shall see in the following section.

6 Block structure and elements of S and W

6.1 THE S MATRIX

Using the orthogonality of ζ_p, ζ_g and ζ_t, expressed by equations (38) and (39), we find that $\mathbf{S}$ is block diagonal. Thus,

$$\mathbf{S}=\begin{bmatrix} S_{pp} & & \\ & S_{gg} & \\ & & S_{tt} \end{bmatrix}. \tag{64}$$

A typical element of the pp block, S_{pp}^{kl} say, is obtained by introducing ζ_p^{k*} and ζ_p^{l} into equation (57) and integrating over the volume of the flux tube. Explicit expressions for the block elements of $\mathbf{S}$ are given in Appendix A2.

6.2 THE W MATRIX

Recalling that $\mathbf{W}=\mathbf{W}(1)+\mathbf{W}(2)+\mathbf{W}(3)$, it is convenient to consider each term separately. In $\mathbf{W}(1)$, only the pp block is non-zero as the p displacements are solely responsible for changes in $\delta\varrho$. Thus,

$$\mathbf{W}(1)=\begin{bmatrix} W_{pp}(1) & & \\ & 0 & \\ & & 0 \end{bmatrix}. \tag{65}$$

Since, $\operatorname{div}\zeta_t=0$ the $\mathbf{W}(2)$ matrix has no contribution from t motions. Its explicit block form is

$$\mathbf{W}(2)=\begin{bmatrix} W_{pp}(2) & W_{pg}(2) & 0 \\ W_{gp}(2) & W_{gg}(2) & 0 \\ 0 & 0 & 0 \end{bmatrix}. \tag{66}$$

Expressions for the block elements are given in the Appendix A4. We note that each term in $\mathbf{W}(2)$ (from equations A9–A12) is proportional to α. For a polytrope of index n, $\alpha=\gamma-(1+1/n)$. A convectively neutral fluid is defined as one in which $\alpha=0$ and, therefore, $\mathbf{W}(2)=0$.

The matrix $\mathbf{W}(3)$ has the following structure

$$\mathbf{W}(3)=\begin{bmatrix} W_{pp}(3) & W_{pg}(3) & 0 \\ W_{gp}(3) & W_{gg}(3) & 0 \\ 0 & 0 & W_{tt}(3) \end{bmatrix} \tag{67}$$

where expressions for the block elements are given in A3. The $\mathbf{W}(3)$ matrix is wholly due to the magnetic field and vanishes when $\mathbf{B}=0$.

Combining equations (65), (66) and (67) gives

$$\mathbf{W} = \begin{bmatrix} W_{pp}(1)+W_{pp}(2)+W_{pp}(3) & W_{pg}(2)+W_{pg}(3) & 0 \\ W_{gp}(2)+W_{gp}(3) & W_{gg}(2)+W_{gg}(3) & 0 \\ 0 & 0 & W_{tt}(3) \end{bmatrix}. \tag{68}$$

7 Block structure of E and Z

The matrix of eigenvalues is by definition block diagonal. Thus,

$$\mathbf{E} = \begin{bmatrix} E_p & & \\ & E_g & \\ & & E_t \end{bmatrix} \tag{69}$$

where each block is itself a diagonal matrix. From equations (65) and (66), we find that there are no mixed *pt* or *gt* blocks in either **S** or **W**. This means that there is no coupling between toroidal motions and *p* or *g* motions. Therefore, **Z** has the following structure

$$\mathbf{Z} = \begin{bmatrix} Z_{pp} & Z_{pg} & 0 \\ Z_{gp} & Z_{gg} & 0 \\ 0 & 0 & Z_{tt} \end{bmatrix}. \tag{70}$$

Two conclusions follow: the first is that there are pure toroidal modes given by

$$W_{tt}Z_{tt} = S_{tt}Z_{tt}E_t \tag{71}$$

and the second is that the remaining modes have both *g* and *p* components, which are solutions of the following equation

$$\begin{bmatrix} W_{pp} & W_{pg} \\ W_{gp} & W_{gg} \end{bmatrix}\begin{bmatrix} Z_{pp} & Z_{pg} \\ Z_{gp} & Z_{gg} \end{bmatrix} = \begin{bmatrix} S_{pp} & 0 \\ 0 & S_{gg} \end{bmatrix}\begin{bmatrix} Z_{pp} & Z_{pg} \\ Z_{gp} & Z_{gg} \end{bmatrix}\begin{bmatrix} E_p & 0 \\ 0 & E_g \end{bmatrix} = 0. \tag{72}$$

Before, attempting a general solution to equations (71) and (72), it is useful to consider some special cases.

8 Special cases

Let us recall the correspondence between various members of the trios we discussed in Section 3. Pressure forces are important if the motions are dominated by the irrotational displacement ζ_p. These contribute to **W**(1). Buoyancy forces, acting through **W**(2), are most effective when the displacements are of the solenoidal poloidal type ζ_g. Magnetic forces, which give rise to **W**(3), are created by all three displacements ζ_p, ζ_g and ζ_t. It may, however, be noted that ζ_t appears only in **W**(3), and may thus be considered as generating motions induced purely by Lorentz forces. To see the interplay of the various terms in **W** and their relative importance with regard to the mode spectrum, we first treat some idealized cases.

8.1 UNSTRATIFIED AND NON-MAGNETIZED MEDIUM

Absence of gravity implies a fluid with uniform density and pressure. Buoyancy is absent and the only non-vanishing contribution in **W** comes from **W**(1). On evaluating the various integrals in **W**(1) and **S**, we obtain the following dispersion relation (see Appendix A4 for details)

$$\omega^2 = l^2 c_s^2 \tag{73}$$

where l and c_s respectively denote the wavenumber and sound speeds given by $l^2=i^2+j^2+k^2$ and $c_s^2=\gamma P_0/\varrho_0$. Equation (73) is the usual dispersion relation for acoustic waves, which are driven by pressure forces. The frequencies increase with mode order, since high mode orders imply steeper pressure gradients. Solenoidal motion of g and t remain neutral.

8.2 UNSTRATIFIED AND MAGNETIZED FLUID

In addition to $\mathbf{W}(1)$, we must now also consider the contribution due to $\mathbf{W}(3)$. The $\mathbf{W}$ matrix in equation (68) takes the following form

$$\mathbf{W}=\begin{bmatrix} W_{pp}(1) & W_{pg}(3) & 0 \\ W_{gp}(3) & W_{gg}(3) & 0 \\ 0 & 0 & W_{tt}(3) \end{bmatrix}. \tag{74}$$

It is readily seen (see A4) that the dispersion relation is

$$(\omega^2-k^2v_a^2)(\omega^4-\omega^2l^2(c_s^2+v_a^2)+k^2l^2c_s^2v_a^2)=0 \tag{75}$$

where v_a is the Alfvén speed given by $v_a=B/\sqrt{4\pi\varrho_0}$. Equating the first factor in equation (75) to zero yields the usual dispersion relation for Alfvén waves. These are pure t motions, uncoupled from the rest, with frequencies which increase with mode order. Similar to p motions, the reason is that the magnetic forces depend on the spatial derivatives of $\delta\mathbf{B}$, which decrease with decreasing wavelength.

Equating the second factor in equation (75) to zero yields the conventional dispersion relation for fast and slow waves, which correspond respectively to the positive and negative roots given by

$$\omega^2=\frac{l^2(c_s^2+v_a^2)}{2}\left[1\pm\sqrt{1-\frac{4k^2c_t^2}{l^2(c_s^2+v_a^2)}}\right] \tag{76}$$

where $c_t=c_sv_a/\sqrt{c_s^2+v_a^2}$. In the limit $k/l\rightarrow 0$, which corresponds to the slender flux tube approximation, the fast and slow mode frequencies are respectively

$$\omega_f^2\approx\frac{l^2(c_s^2+v_a^2)}{2} \tag{77}$$

$$\omega_s^2\approx k^2c_t^2. \tag{78}$$

Equation (78) is also the dispersion relation for a slender flux tube (Roberts & Webb 1978), which suggests that the normal mode is essentially a slow mode propagating with the 'tube speed' c_t. For both fast and slow modes, the frequency increases with mode number. Slow modes have one important property in common with g modes of a stratified fluid; in both the dominant component is the solenoidal poloidal vector ζ_g. Similarly, the fast modes resemble p modes due to a large contribution from the ζ_p component.

9 Stratified fluid

We now consider the general case of a stratified fluid in the presence of a magnetic field. Owing to the mathematical complexity of the problem it is convenient to attempt a numerical solution to the generalized eigenvalue problem.

9.1 NUMERICAL METHOD

A Rayleigh–Ritz variational scheme was adopted to solve equations (71) and (72). We approximate the linear series in equation (55) by a finite number of terms, say n. The matrices entering in

Table 1. The frequency ω^2 for different modes and orders in an unstratified magnetized medium, assuming $v_a^2/c_s^2=1.5$, $\gamma=5.3$ and $i=j=10$.

	k				
Mode	1	2	3	4	5
g	0.834	3.35	7.58	13.6	21.4
t	1.00	4.00	9.00	16.0	25.0
p	669	677	689	706	729

equations (71) and (72) are truncated to $n\times n$. We solve these equations using standard algorithms for generalized eigenvalue problems. Briefly, the method consists of using a sequence of unitary transformations to convert the **W** and **S** matrices into quasi-triangular and upper triangular forms respectively. Eigenvalues (ω^2) can now be most conveniently extracted. The method also determines the eigenvectors (i.e. the variational parameters **Z**). We calculate the integrals, appearing in the **W** and **S** matrices, using Simpson's rule. In the computations, up to a maximum of 26 variational parameters were used, 13 for each of the p and g terms.

We checked our numerical procedure by firstly treating the case of an unstratified magnetized fluid, which was discussed in the previous section. Results are shown in Table 1, where ω^2 is tabulated for the first five modes, assuming $\gamma=5/3$, $v_a^2/c_s^2=1.5$ and $i=j=10$. (Henceforth, we shall implicitly assume $i=j$.) Frequencies are in units of $\omega_0=\sqrt{P_0/l_0^2\varrho_0}=\sqrt{\pi^2P_0/d^2\varrho_0}$, where l_0 is the unit of length and chosen such that $l_0=d/\pi$. A comparison with equation (75), shows perfect agreement for all the modes (p, g, t).

In the following sections, we shall consider various cases of possible physical interest.

9.2 STRATIFIED NON-MAGNETIC FLUID

The matrix **W** has contributions from both **W**(1) and **W**(2). When the motions have a large ζ_p component, **W**(1) dominates, whereas **W**(2) is important for motions with large ζ_g. Due to the non-vanishing of the off-diagonal block of **W**(2), there is an interaction between ξ_p and ζ_g motions; one excites the other. The modes exhibit the well-known bispectral feature, which may be seen in Fig. 1. Plotted is the variation with k (vertical mode number) of ω^2 for both p and g

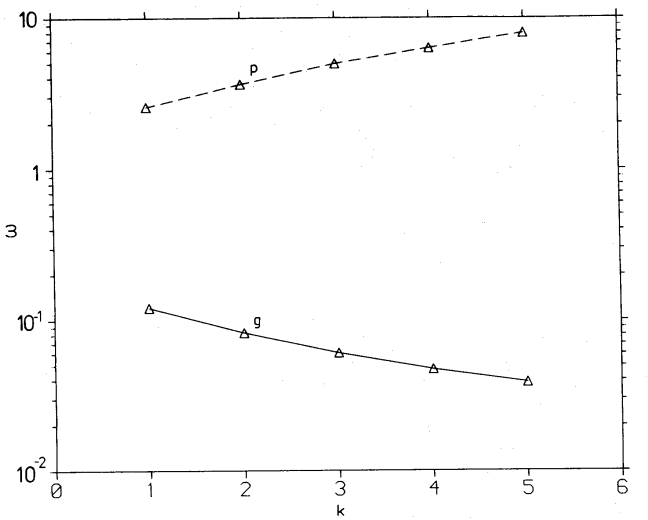

Figure 1. Variation of the dimensionless frequency ω with k for $n=2.0$, $h=0.5$, $i=1$ and $\gamma=5/3$. Solid and dashed lines correspond to g and p modes respectively.

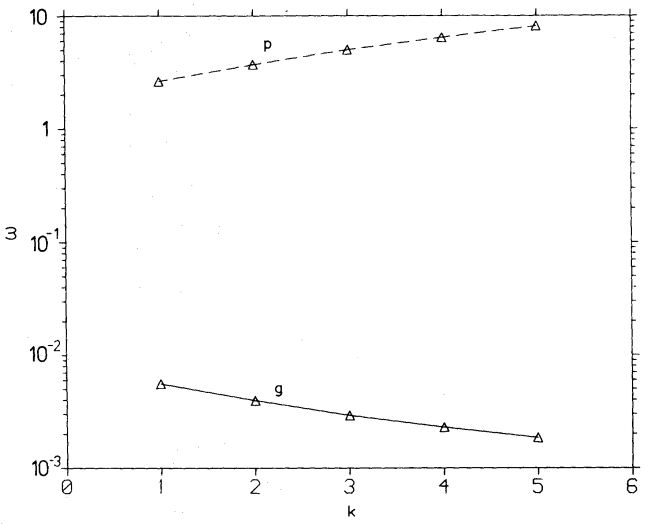

Figure 2. Frequency-dependence of g and p modes (solid and dashed lines respectively) with k for an unmagnetized and almost convectively neutral fluid ($n=1.501$), assuming $h=0.5$, $\gamma=5/3$ and $i=1$.

modes assuming $h=0.5$, $n=2$, $\gamma=5/3$ and $i=1$ (the pressure scale height h is measured in units of l_0). The p spectrum has a sequence of increasing frequencies with mode order, for reasons already explained. The g frequencies decrease with k, accumulating at zero. This is due to the nature of buoyancy, which is a body force that becomes vanishingly small for perturbations with decreasing wavelength or increasing wavenumber. Mathematically, the behaviour of p mode and g mode frequencies is related to the sturmian and anti-sturmian properties respectively of the modes (Roberts 1985). Toroidal motions remain neutral in non-magnetic fluids.

It is tempting to consider the case of a convectively neutral fluid ($\alpha=0$), for which $\mathbf{W}(2)=0$. In such a fluid, only acoustic (p) modes can occur; the g and t motions are neutral. If $\alpha\neq0$, but is small, g motions are also excited. Up to order α^2, however, they remain purely of ζ_g type (Sobouti & Silverman 1978). In the present problem, this can be seen from equation (72), by expanding W_{pg}, W_{gp}, W_{gg} and E_g in powers of α and retaining only first-order terms. We can, therefore,

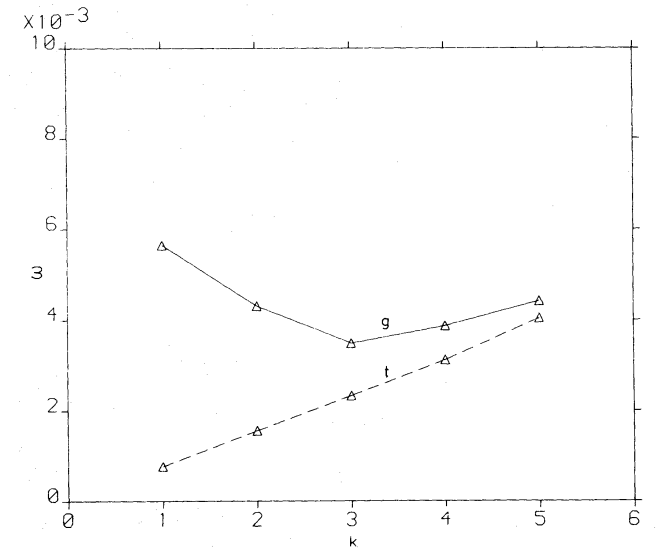

Figure 3. Frequency-dependence of g (solid lines) and t (dashed lines) modes with k for a weakly magnetized ($B^2/4\pi P_0=10^{-6}$) and almost convectively neutral fluid ($n=1.501$) assuming $h=0.5$, $\gamma=5/3$ and $i=1$.

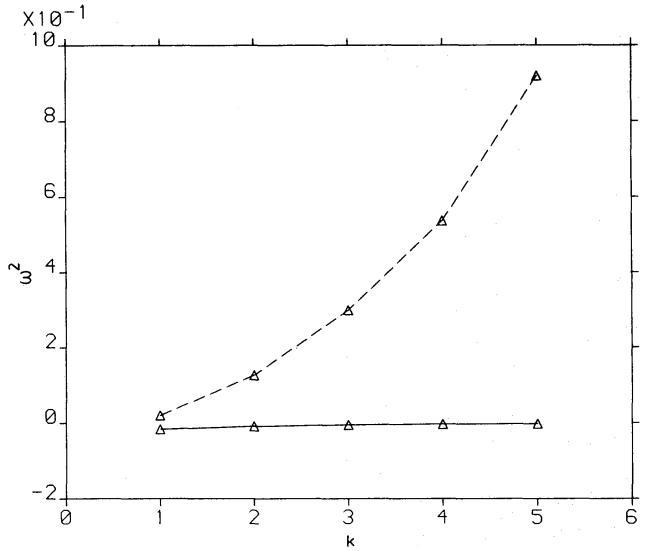

Figure 4. Frequency-dependence of g modes with k, for a convectively unstable fluid ($\alpha<0$), assuming $n=1.0$, $h=0.5$, $\gamma=5/3$ and $i=1$. Solid and dashed lines correspond to $B=0$ and $B^2/4\pi P_0=0.05$ respectively.

conclude that a slightly convectivley non-neutral fluid has pure p and g spectra. The frequency behaviour is shown in Fig. 2 for $n=1.501$ and $h=0.5$ (other parameters remain unchanged).

Let us now consider the effect of a small magnetic field on an equilibrium which is slightly convectivley non-neutral. Fig. 3 shows the g and t modes for $B^2/4\pi P_0=10^{-6}$. The simplest to understand is the toroidal spectrum, which consists of standing Alfvén waves. We have not plotted the acoustic or p branch, as it is the same as the unmagnetized case shown in Fig. 2. However, the g spectrum is completely different than before. It appears, that the introduction of even a minute magnetic field can entirely alter the ω–k dependence. The short-wavelength limit behaves like the slow spectrum of an unstratified magnetized medium. On the other hand, the long-wavelength limit is similar to the g spectrum of a stratified unmagnetized fluid. This explains the peculiar form of the spectrum, in which ω^2 first decreases with k, but subsequently increases with k, when magnetic forces become dominant. There is no frequency accumulation at zero for large k.

The case of a convectively unstable medium is also interesting. In the absence of a magnetic field, it has a sequence of negative eigenvalues ($\omega_g^2<0$), with an accumulation point at zero. Fig. 4 shows ω_g^2 as a function of k for an unmagnetized ($B=0$) and magnetized fluid ($B^2/4\pi P_0=0.05$), shown in full and dashed lines respectively, assuming $n=1.0$. We find that a modest field can completely transform an unstable g spectrum and replace it with a slow spectrum, which is stable. The stabilizing effect of the magnetic field enters through $\mathbf{W}(3)$ (proportional to B^2), which is always positive.

10 Intense flux tubes

We now consider a range of parameters that may be applicable to intense flux tubes on the Sun. Let us choose the level $z=0$, to correspond to the height in the photosphere where the (continuum) optical depth is unity. The polytropic index n is not a constant, but varies from about 1.0 near the surface to about 3.3 at a depth of a few hundred kilometres. In order to compare our results with those of Webb & Roberts (1978) for a slender flux tube, we take $n=2.3$, $h=0.076$, $d=2000$ km, $\beta=2/\gamma$ [corresponding to their choice of $\Lambda_0'=-0.3$, $\Lambda_0(0)=P_0/\varrho_0 g=152$ km and $v_a^2(0)/c_s^2(0)=1$], $\gamma=1.2$ and $i=10$. The latter value ensures that we are dealing with a tube of

Table 2. The frequency $\omega^2(s^{-2})$ for different modes and orders in an intense flux tube, assuming $n=2.3$, $h=0.076$, $d=2000$ km, $\gamma=1.2$, $\beta=2/\gamma$ and $i=10$.

	k		
Mode	1	2	3
g	-6.04×10^{-5}	-1.73×10^{-5}	3.40×10^{-5}
t	6.73×10^{-6}	3.63×10^{-5}	8.40×10^{-5}
p	5.37×10^{-2}	5.93×10^{-2}	6.76×10^{-2}

thickness a, which is much less than its length d. Table 2 shows the eigenfrequencies of the first three g, t and p modes obtained as a result of using 26 variational parameters (i.e. $k_{max}=13$). As already discussed in Section 8.1, the relevant mode which should be compared is the g_1 mode. This is essentially a convective mode, modified by the magnetic field with a growth rate $7.7\times10^{-3}\,s^{-1}$. Webb & Roberts found a maximum growth rate $5.3\times10^{-3}\,s^{-1}$, which appears to be in reasonable agreement with our result, considering that their equilibrium had $T=T_e$, in contrast to $\varrho=\varrho_e$, assumed by us. They, however, briefly discussed, without actual calculation, the latter case and showed that a sufficient condition for stability is the same as the criterion found by Gough & Tayler (1966).

Fig. 5 shows a plot of the frequency as a function of the mode number k for the g, t and p modes, assuming $n=1.0$ and $i=5$ (other parameters remaining the same). The branch for the g modes starts at $k=2$, as the lowest order mode is unstable. For low orders, the frequencies are well separated, but as k increases the t (Alfvén) and g branches become practically indistinguishable (for low values of n). The reason for this is because at high values of k, the g mode is essentially a slow mode, with a phase speed approximately the Alfvén speed (c_s increases with z faster than v_a). At high k, the p mode is an acoustic mode travelling with a phase speed $c_s>v_a$. This explains why the p branch remains quite distinct from the other two branches. In the actual computations, we did not encounter practical difficulties in the determination of the g and t modes, when their frequencies became very close, because we used two separate equations (equations 71 and 72).

We now turn our attention to the behaviour of the eigenfunctions, corresponding to the eigenvalues shown in Fig. 5. In Fig. 6(a–d), the variation of ξ_{pz}, ξ_{gz}, δP_p and δP_g with depth

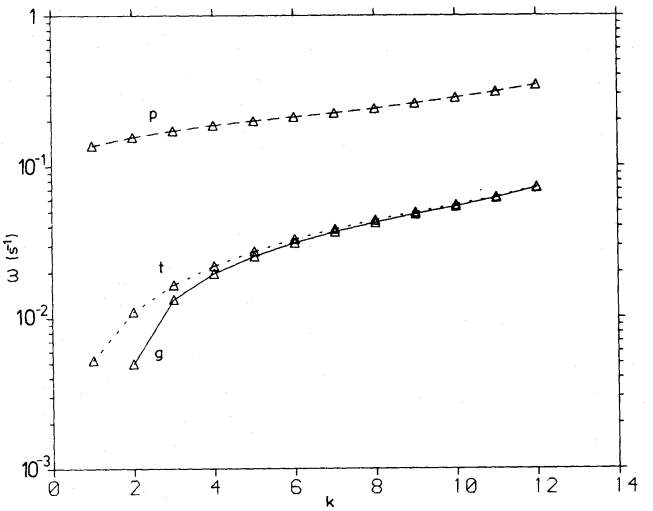

Figure 5. Variation of $\omega(s^{-1})$ with k in an intense flux tube, assuming $n=1.0$, $h=0.076$, $\gamma=1.2$, $\beta=2/\gamma$, $d=2000$ km and $i=5$. The g, t and p branches are explicitly marked in the diagram.

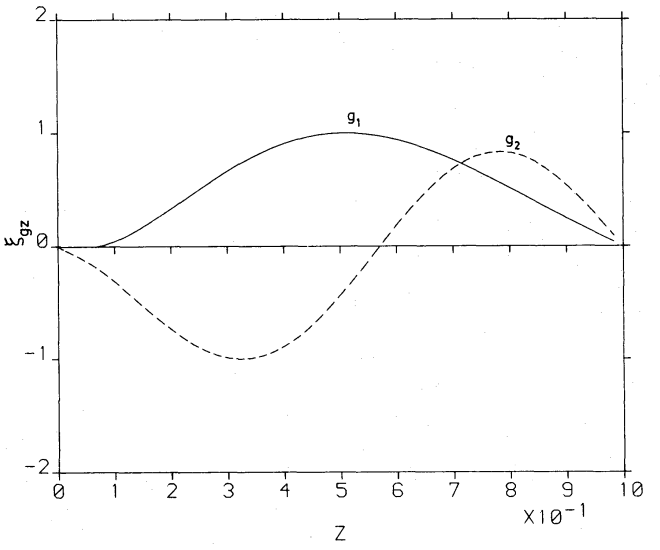

(a)

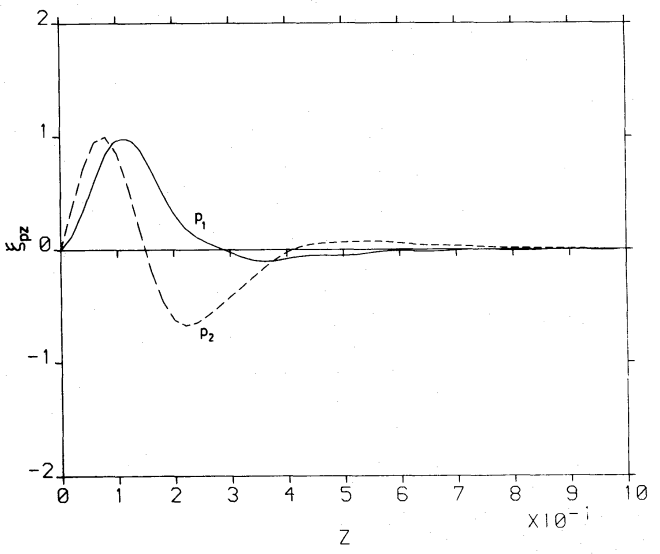

(b)

Figure 6. Variation parallel to the tube axis with depth z (in units of d) of the (a) vertical displacement in g motions (ξ_{gz}), (b) vertical displacement in p motions (ξ_{pz}), (c) relative Eulerian perturbations in pressure in g motions ($\delta P_g/P$), (d) relative Eulerian perturbations in pressure in p motions ($\delta P_p/P$), assuming the same parameters as in Fig. 5. The solid and dashed lines correspond to the first and second mode orders.

(measured in units of d) along the z axis are shown for the lowest two orders ($k=1, 2$). All quantities are normalized with respect to their maximum values in the interval $(0, \pi)$. The main difference in the behaviour of the displacement ξ_z for the g and p modes is that the former has a substantial contribution over the entire height range, whereas the latter is more or less confined to the upper regions of the tube. In the conventional terminology, the g_1 mode, with no node, could be identified as the fundamental. It is an unstable g mode, which occurs when N^2, where N is the Brunt–Väisälä frequency, becomes negative. The localization of the p modes to the top layers of the tube, suggests the presence of a cavity. An acoustic wave propagating downwards into a region of increasing sound speed, suffers refraction until its vertical wavenumber becomes zero. Beyond this point, the wave is evanescent, which mathematically corresponds to a sharp decrease

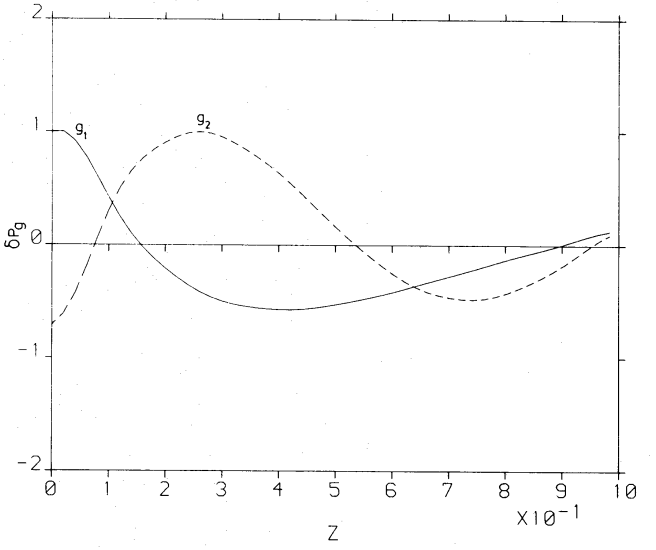

(c)

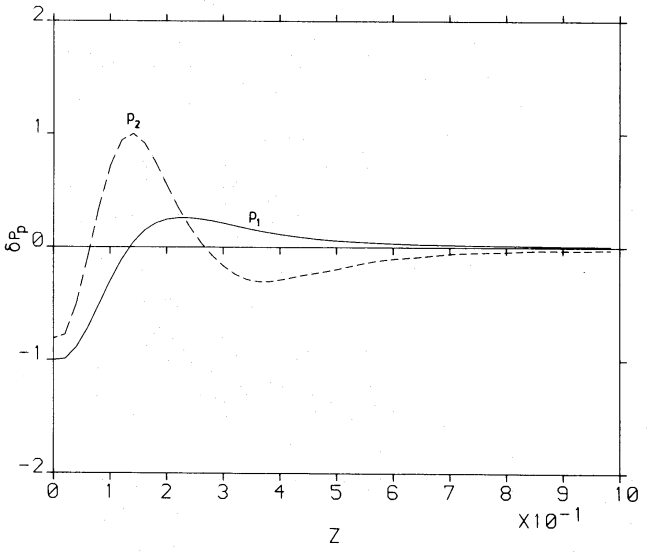

(d)

Figure 6 – *continued*

in wave amplitude with depth. Acoustic waves, with large horizontal wavenumber (large i), suffer appreciable refraction and consequently do not penetrate deep layers. We have also plotted the Eulerian changes in pressure associated with the $p_{1,2}$ and $g_{1,2}$ modes. It might be noted that all the eigenvectors are arbitrary to a multiplicative constant. Thus, it is not possible to say anything about their relative magnitudes. However, by looking at the z variation, we find that the local phase difference between δP and ξ_z, for both modes, changes with z, owing to the stratification. For the g modes, δP and ξ_z appear to be anti-correlated, with the phase difference increasing with z from about $\pi/2$, near the top, to some value below π in the deeper layers. The variation of δP and ξ_z for the p modes close to the surface appears to be correlated. We can correlate δP with ϱv_z, by recalling that the latter has a phase difference of $\pi/2$ with ξ_z.

Let us finally consider the effect of varying the horizontal mode number (i), the polytropic index (n) and the magnetic field (β) on the eigenfrequencies. The results are presented in Tables

Table 3. The lowest order frequency $\omega^2(s^{-2})$ of the g and p modes for various i, assuming $n=1.0$ and $\beta=2/\gamma$.

	i		
Mode	1	5	10
g	-1.88×10^{-5}	-4.93×10^{-5}	-6.01×10^{-5}
p	3.62×10^{-3}	1.58×10^{-2}	5.37×10^{-2}

Table 4. The frequency $\omega^2(s^{-2})$ of the lowest order g, t and p modes for various n, assuming $\beta=2/\gamma$ and $i=5$.

	n		
Mode	1.0	1.8	2.3
g	-7.66×10^{-5}	-5.70×10^{-5}	-4.93×10^{-5}
t	2.77×10^{-5}	1.10×10^{-5}	6.73×10^{-6}
p	1.89×10^{-2}	1.68×10^{-2}	1.58×10^{-2}

Table 5. The frequency ω^2 of the lowest order g, t and p modes for different β, assuming $n=1.0$ and $i=5$.

	β		
Mode	1.5	3.0	10.0
g	-6.87×10^{-5}	-1.17×10^{-4}	-1.82×10^{-4}
t	3.07×10^{-5}	1.54×10^{-5}	4.61×10^{-6}
p	1.94×10^{-2}	1.68×10^{-2}	1.51×10^{-2}

3–5. We find that lowering n has a destabilizing effect on the convective modes (i.e. the low-order g modes), due to an increase in the buoyancy force. However, increasing n or decreasing β has a stabilizing influence, owing to a decrease in superadiabaticity (through larger α) and increase in magnetic field strength respectively. In order to understand the effect of varying n on the t and p modes, let us note that at a fixed depth in the tube, $d\varrho/dn>0$ and $dT/dn<0$ (for fixed ϱ_0 and T_0), and thus the Alvén speed and sound speeds increase and decrease respectively with increasing n. These, however, are the phase speeds of the t and p modes, thus explaining the trend in Table 4. We have omitted the t modes in Table 3, since they have no i-dependence (their frequencies are proportional only to k). The p-mode frequencies are proportional to the total wavenumber ($\sqrt{i^2+j^2+k^2}$) and increase with i. Lastly, increasing the magnetic field (or decreasing β) increases the Alfvén speed and consquently the frequencies of the t and to some extent of the p modes (see equation 77).

11 Discussion and observational implications

We have used a gauged version of Helmholtz's theorem, following Sobouti (1981), to classify the various types of wave motions that can occur in a magnetized fluid. The decomposition of the perturbations into p, g and t components has a physical basis (related to the various forces present in the fluid), thereby, greatly simplifying the task of mode identification. In practical terms, decoupling the equation for the t modes is greatly advantageous, since the frequencies of the Alfvén and slow waves can become very close. We should also once again remind the reader that

the notation p and g does not correspond to the conventional one, as used in helioseismology (see review by Deubner & Gough 1984 on the conventional p- and g-mode nomenclature), and may not adequately describe the nature of a MAG wave. It is, however, used because it reflects the fact that the dominant contribution to an eigensolution, say ξ_p, comes from ζ_p motions.

In the analysis, we made a number of simplifying assumptions. We neglected the pressure perturbation in the external medium, thus eliminating any dynamical coupling between the medium and the flux tube. This coupling, will in general, not only excite surface modes, but also alter the spectrum of body waves. The problem for an unstratified medium has been treated fairly exhaustively by Roberts (1981a, b; see also Roberts & Webb 1979; Edwin & Roberts 1982, 1983; Cally 1985a, b). For typical photospheric conditions, the essential modification due to inclusion of the external perturbation, is that the slow body wave propagates with a higher phase speed (between c_t and v_a) than before. The fast body wave also travels with a higher speed (between c_s and c_{se}, the sound speeds in the tube and external medium respectively). In addition, there is a slow surface mode with phase speed lower than c_t. If the external gas is only slightly hotter than the gas inside the flux tube, the fast body wave speed is almost unchanged. Furthermore, when the flux tube is sufficiently thin, both the surface and body waves have approximately the same phase speed. It thus appears that neglecting the external perturbation may be a reasonable approximation for a thin flux tube, which has comparable temperature with the external medium. A rigorous calculation which treats this effect for the stratified case, would still be desirable.

Another approximation that we made was the assumption of a uniform magnetic field. This assumption is unlikely to be correct, as we expect the field to increase with depth, so that the tube narrows in cross-section with depth. Thus, we underestimate the Alfvén speed and neglect the tension in the field, both of which will change the frequency spectrum. These effects will be considered elsewhere.

Let us now consider some of the observational implications of our results. We found that for flux tubes, extending vertically downward from the surface into the convection zone, there exists typically one unstable mode (g_1) with a growth rate of a few hundred seconds. The consequences of this on the formation of flux tubes, through convective collapse have been explored in detail elsewhere (Hasan 1984a, b). Higher order g modes are stable with frequencies increasing with mode number and with values which are close to those of the Alfvén (t) modes. The p modes have much higher frequencies, corresponding to periods which are typically of the order of seconds. Regarding the eigenfunctions, we find that the g modes penetrate deep into the tube and are, therefore, influenced by physical conditions existing over the entire extension of the tube. The high i (≥ 5) p modes have a significant contribution from a comparatively smaller height range, and provide a useful diagnostic for probing the surface layers, similar to the global p modes, whereas the g modes can reveal information about the deeper layers. The p modes of a thin flux tube, however, have much higher frequencies than their global counterparts. Unfortunately, it is difficult using present ground-based observational techniques, to detect oscillations in intense flux tubes; thus a comparison must await a future date. On the basis of our fairly simple model, it does not seem worthwhile to make detailed predictions. Nevertheless, we hope that our calculations provide some worthwhile information on the character of wave modes in intense flux tubes. We are in the process of refining our calculations by considering an equilibrium stratification based on a model atmosphere and choosing a tapered flux tube of circular cross-section. The results of this investigation will be communicated in a forthcoming publication.

12 Concluding remarks

The purpose of this study was to delineate the type of motions that can occur in a stratified flux tube. We have used a convenient technique which allows a natural classification of the modes.

Our p modes are associated with motions that are mainly irrotational. The g and t modes correspond to solenoidal motions which are poloidal and toroidal respectively. We considered some special cases to study the property of the different modes. In the absence of a magnetic field, the p and g modes can be identified with modes that are mainly pressure- and gravity-driven respectively. However, when a magnetic field is present, a straightforward interpretation of p and g modes is not always obvious. The former can usually be considered as a gravity-modified fast mode and the latter as a gravity-modified slow mode at high frequencies. At intermediate frequencies, the g modes can exhibit a peculiar behaviour, when they neither resemble pure gravity nor slow modes. For low mode orders and weak magnetic fields, the g modes behave as conventional gravity modes. In the short-wavelength limit, however, gravity plays only a subsidiary role and the g modes are essentially slow wave for all mode orders. The t modes can always be identified with Alfvén waves.

We have considered a range of parameters, typical of conditions in the sub-photospheric layers of the Sun. This allows us to approximately determine the frequencies and the height variation of the perturbations in intense flux tubes. Such information is potentially important as a diagnostic for finding out more about physical conditions in such tubes. Although, it is still premature to make predictions on the precise frequencies that one could detect in fibrils, our study gives a broad range of values in which the actual observations would lie. Calculations, that are presently underway, are likely to provide values that could be used as a basis for comparison.

Acknowledgments

We are grateful to Professor A. Salam for inviting us to the International Centre for Theoretical Physics, Trieste where this work was initiated. Financial support was provided by the Science and Engineering Research Council, UK to SSH and by the Research Council of Shiraz University to YS. We thank Dr S. J. Schwartz for reading the manuscript and making helpful comments.

References

Antia, H. M. & Chitre, S. M., 1978. *Solar Phys.*, **63,** 67.
Bel, N. & Mein, P., 1971. *Astr. Astrophys.*, **11,** 234.
Cally, P. S., 1985a. *Solar Phys.*, **103,** 277.
Cally, P. S., 1985b. *Aust. J. Phys.*, **38,** 825.
Chandrasekhar, S., 1964. *Astrophys. J.*, **139,** 664.
Cram, L. E. & Wilson, P. R., 1975. *Solar Phys.*, **41,** 313.
Defouw, R. J., 1976. *Astrophys. J.*, **209,** 266.
Deubner, F.-L. & Gough, D. O., 1984. *Ann. Rev. Astr. Astrophys.*, **22,** 593.
Edwin, P. M. & Roberts, B., 1982. *Solar Phys.*, **76,** 239.
Edwin, P. M. & Roberts, B., 1983. *Solar Phys.*, **88,** 179.
Ferraro, V. C. A. & Plumpton, C., 1966. *An Introduction to Magneto-Fluid Mechanics,* 2nd edn, Clarendon Press, Oxford.
Giovanelli, R. G., 1975. *Solar Phys.*, **44,** 299.
Giovanelli, R. G., Harvey, J. W. & Livingston, W. C., 1978. *Solar Phys.*, **59,** 40.
Gough, D. O. & Tayler, R. J., 1966. *Mon. Not. R. astr. Soc.*, **133,** 85.
Hasan, S. S., 1984a. *Astrophys. J.*, **285,** 851.
Hasan, S. S., 1984b. *Astr. Astrophys.*, **143,** 39.
Hasan, S. S., 1986. *Mon. Not. R. astr. Soc.*, **219,** 357.
Lighthill, M. J., 1967. *IAU Symp. No. 28*, p. 429, Reidel, Dordrecht, Holland.
Lites, B. W. & Thomas, J. H., 1985. *Astrophys. J.*, **294,** 682.
McLellan, A. & Winterberg, F., 1968. *Solar Phys.*, **4,** 401.
Moore, R. L., 1981. *Space Sci. Rev.*, **28,** 387.
Nagakawa, Y., Priest, E. R. & Wellck, R. E., 1973. *Astrophys. J.*, **184,** 931.
Parker, E. N., 1974. *Solar Phys.*, **37,** 127.

Parker, E. N., 1978. *Astrophys. J.*, **211,** 368.
Roberts, B., 1981a. *Solar Phys.*, **69,** 27.
Roberts, B., 1981b. *Solar Phys.*, **69,** 39.
Roberts, B., 1985. In: *Solar System Magnetic Fields,* Chap. 3, ed. Priest, E. R., Reidel, Dordrecht, Holland.
Roberts, B. & Webb, A. R., 1978. *Solar Phys.*, **56,** 5.
Roberts, B. & Webb, A. R., 1979. *Solar Phys.*, **64,** 77.
Schwartz, S. J. & Bel, N., 1984. *Astr. Astrophys.*, **137,** 218.
Sobouti, Y., 1977a. *Astr. Astrophys.*, **55,** 327.
Sobouti, Y., 1977b. *Astr. Astrophys.*, **55,** 339.
Sobouti, Y., 1981. *Astr. Astrophys.*, **100,** 319.
Sobouti, Y., 1986. *Astr. Astrophys.*, **169,** 95.
Sobouti, Y. & Silverman, J. N., 1978. *Astr. Astrophys.*, **62,** 365.
Spruit, H., 1979. *Solar Phys.*, **61,** 363.
Spruit, H., 1982. *Astr. Astrophys.*, **75,** 3.
Spruit, H. & Zweibel, E., 1979. *Astr. Astrophys.*, **62,** 15.
Stenflo, J. O., 1973. *Solar Phys.*, **32,** 41.
Thomas, J. H., 1982. *Astrophys. J.*, **262,** 760.
Webb, A. R. & Roberts, B., 1978. *Solar Phys.*, **59,** 249.
Wentzel, D. G., 1979. *Astr. Astrophys.*, **76,** 20.
Wilson, P. R., 1979. *Astr. Astrophys.*, **71,** 9.
Zhugzhda, Y. & Dzhalilov, N., 1984. *Astr. Astrophys.*, **132,** 145.

Appendix

A1 DIAGONALIZATION OF **W** AND **S** BY **Z**

We prove the assertion that a matrix **Z** exists, which simultaneously diagonalizes **W** to **E** and **S** to **I** (i.e. equations 62a, b).

Left multiplication of equation (56) by $\mathbf{Z}^+$ gives

$$\mathbf{Z}^+\mathbf{W}\mathbf{Z}=\mathbf{Z}^+\mathbf{S}\mathbf{Z}\mathbf{E}. \tag{A1}$$

The Hermitian adjoint of equation (56) is

$$\mathbf{Z}^+\mathbf{W}=\mathbf{E}^+\mathbf{Z}^+\mathbf{S}, \tag{A2}$$

where we have used the property that **W** and **S** are real. Inserting equation (A2) in equation (A1), yields

$$\mathbf{E}^+\mathbf{Z}^+\mathbf{S}\mathbf{Z}-\mathbf{Z}^+\mathbf{S}\mathbf{Z}\mathbf{E}=0. \tag{A3}$$

A diagonal element *ii* of equation (A3) is

$$(\varepsilon_i^*-\varepsilon_i)(\mathbf{Z}^+\mathbf{S}\mathbf{Z})_{ii}=0$$

since **E** and $\mathbf{E}^+$ are diagonal. This leads to the relation $\varepsilon_i^*=\varepsilon_i$, so that ε_i is real. Next, let us consider an off-diagonal element *ij* of equation (A3)

$$(\varepsilon_i-\varepsilon_j)(\mathbf{Z}^+\mathbf{S}\mathbf{Z})_{ij}=0.$$

If $\varepsilon_i\neq\varepsilon_j$, we conclude that

$$(\mathbf{Z}^+\mathbf{S}\mathbf{Z})_{ij}=0. \tag{A4}$$

In the degenerate case, $\varepsilon_i=\varepsilon_j$ and the conclusion does not follow. There is, however, enough freedom to impose it within the subspace of the degenerate eigenvalues by, say, a Schmidt orthogonalization. This proves relation (62b). Substituting this relation in equation (A1) gives the other relation (62a). *Q.E.D.*

A2 MATRIX ELEMENTS OF **S**

We can carry out the x and y integrations that appear in equation (57) analytically. Using equations (41), (46) and (51) gives

$$S^{kl}_{pp}=\frac{2}{\pi}\varrho_0\int_0^{\pi}\frac{\varrho}{\varrho_0}\left[(i^2+j^2)\cos(kz)\cos(lz)+kl\sin(kz)\sin(lz)\right]dz \tag{A5}$$

$$S^{kl}_{gg}=\frac{2}{\pi}(i^2+j^2)\varrho_0\int_0^{\pi}\frac{\varrho_0}{\varrho}\left[kl\cos(kz)\cos(lz)+(i^2+j^2)\sin(kz)\sin(lz)\right]dz \tag{A6}$$

$$S^{kl}_{tt}=\frac{2}{\pi}(i^2+j^2)\varrho_0\int_0^{\pi}\frac{\varrho}{\varrho_0}\cos(kz)\cos(lz)\,dz. \tag{A7}$$

A3 MATRIX ELEMENTS OF **W**

Performing the integrations in equations (59), (60) and (61) and using equations (40)–(54) yields

$$W^{kl}_{pp}(1)=\frac{2}{\pi}\int_0^{\pi}\varrho\frac{dP}{d\varrho}\left[(i^2+j^2+k^2)\cos(kz)+\frac{\varrho'}{\varrho}k\sin(kz)\right]\times\left[(i^2+j^2+l^2)\cos(lz)+\frac{\varrho'}{\varrho}l\sin(lz)\right]dz \tag{A8}$$

$$W^{kl}_{pp}(2)=\frac{2}{\pi}(i^2+j^2+k^2)(i^2+j^2+l^2)\int_0^{\pi}\alpha P\cos(kz)\cos(lz)\,dz \tag{A9}$$

$$W^{kl}_{pg}(2)=-\frac{2}{\pi}(i^2+j^2+k^2)(i^2+j^2)\varrho_0\int_0^{\pi}\alpha P\frac{\varrho'}{\varrho^2}\cos(kz)\sin(lz)\,dz \tag{A10}$$

$$W^{lk}_{gp}(2)=W^{kl}_{pg}(2) \tag{A11}$$

$$W^{kl}_{gg}(2)=\frac{2}{\pi}(i^2+j^2)^2\varrho_0^2\int_0^{\pi}\alpha P\frac{\varrho'^2}{\varrho^4}\sin(kz)\sin(lz)\,dz \tag{A12}$$

$$W^{kl}_{pp}(3)=\frac{B^2}{4\pi}(i^2+j^2)(i^2+j^2+k^2)\,\delta_{kl} \tag{A13}$$

$$W^{kl}_{pg}(3)=-\frac{B^2}{2\pi^2}(i^2+j^2)l\int_0^{\pi}\left(\frac{\varrho_0}{\varrho}\right)\times\left\{k\sin(kz)\left[l\sin(lz)+\frac{\varrho'}{\varrho}\cos(lz)\right]+(i^2+j^2)\cos(kz)\cos(lz)\right\}dz \tag{A14}$$

$$W^{lk}_{gp}(3)=W^{kl}_{pg}(3) \tag{A15}$$

$$W^{kl}_{gg}(3)=\frac{B^2}{2\pi^2}(i^2+j^2)kl\int_0^{\pi}\left(\frac{\varrho_0}{\varrho}\right)^2\left\{\left[k\sin(kz)+\frac{\varrho'}{\varrho}\cos(kz)\right]\left[l\sin(lz)+\frac{\varrho'}{\varrho}\cos(lz)\right]+(i^2+j^2)\cos(kz)\cos(lz)\right\}dz \tag{A16}$$

$$W^{kl}_{tt}(3)=\frac{B^2}{4\pi}(i^2+j^2)\,k^2\delta_{kl}. \tag{A17}$$

A4 DISPERSION RELATION FOR AN UNSTRATIFIED FLUID

For an unstratified fluid, the z integrals appearing in S_{ij} and W_{ij}, where $i, j=p, g, t$ become trivial. The only non-vanishing elements are $W^{kl}_{pp}(3)$ given by equation (A13), $W^{kl}_{tt}(3)$ given by equation (A17) and

$$W^{kl}_{pp}(2)=(i^2+j^2+k^2)^2\ \gamma P_0\ \delta_{kl} \tag{A18}$$

$$W^{kl}_{pg}(3) = W^{lk}_{gp}(3) = -\left(\frac{B^2}{4\pi}\right)(i^2+j^2)(i^2+j^2+k^2)\ k\delta_{kl} \tag{A19}$$

$$W^{kl}_{gg}(3) = \left(\frac{B^2}{4\pi}\right)(i^2+j^2)(i^2+j^2+k^2)\ k^2\delta_{kl} \tag{A20}$$

$$S^{kl}_{pp}=\varrho_0(i^2+j^2+k^2)\ \delta_{kl} \tag{A21}$$

$$S^{kl}_{gg}=\varrho_0(i^2+j)(i^2+j^2+k^2)\ \delta_{kl} \tag{A22}$$

$$S^{kl}_{tt}=\varrho_0(i^2+j^2)\ \delta_{kl}. \tag{A23}$$

From equations (71) and (72), we find that the condition for a non-trivial solution is

$$(W_{pp}-\omega^2 S_{pp})(W_{gg}-\omega^2 S_{gg})-W_{pg}W_{gp}=0 \tag{A24}$$

and

$$W_{tt}-\omega^2 S_{tt}=0 \tag{A25}$$

where $W_{pp}=W_{pp}(2)+W_{pp}(3)$, $W_{gg}=W_{gg}(3)$ and $W_{pg}=W_{gp}=W_{pg}(3)$. On substituting equations (A13) and (A17)–(A23) in (A24) and (A25), we obtain the following relations

$$[\omega^4-\omega^2 l^2(c_s^2+v_a^2)+k^2 l^2 c_s^2 v_a^2]=0 \tag{A26}$$

$$(\omega^2-k^2 v_a^2)=0 \tag{A27}$$

where $c_s^2=\gamma P_0/\varrho_0$ and $v_a^2=B^2/4\pi\varrho_0$. For an unmagnetized fluid, $B=0$ and equation (A26) yields the following relation

$$\omega^2 = c_s^2 l^2. \tag{A28}$$

Note added in proof

The vanishing of the third surface term of equation (24), $(\mathbf{B}\cdot\mathbf{n})\ (\boldsymbol{\xi}\cdot\delta\mathbf{B})$, can best be seen through the ansatz of Section 4. This expression vanishes on the flux tube on account of $\mathbf{n}\cdot\mathbf{B}=0$. It vanishes on the planes $z=0$ and d for p and t motions on account of the ansatz of equations (41), (44) and (51), (54). It vanishes for g motions if $\varrho'=0$ on these planes; see the g ansatz of equations (46) and (49). For the sake of simplicity, however, we have left out this last refinement in our calculations for polytropes.